RSC Advances

PAPER

View Article Online
View Journal | View Issue

Cite this: *RSC Adv.*, 2021, **11**, 39978

Polymyxin B engineered polystyrene-divinylbenzene microspheres for the adsorption of bilirubin and endotoxin†

Kangle Yang,[acef] Yaotian Peng,[abd] Lin Wang *[bd] and Li Ren *[abcef]

Received 6th September 2021
Accepted 30th November 2021

DOI: 10.1039/d1ra06684f

rsc.li/rsc-advances

Hemoperfusion is an important strategy for liver disease treatment. Polystyrene-divinylbenzene (PS-DVB) microspheres are widely applied as absorbents in hemoperfusion to efficiently remove the important toxin bilirubin. However, as another common toxin, endotoxin will remain during this process and cause endotoxemia. Therefore, simultaneous removal of both bilirubin and endotoxin is highly desirable. In the present study, we engineered PS-DVB microspheres with polymyxin B sulfate (PMB) to meet this goal. After modification, the novel PMB-engineered (P-PMB) microspheres displayed excellent biocompatibility and hemocompatibility. Notably, compared to PS-DVB microspheres, P-PMB microspheres exhibited markedly stronger detoxification of both bilirubin and endotoxin, increasing by 17.03% and 42.57%, respectively. Overall, we believe that the novel P-PMB microspheres have considerable potential for liver disease treatment in clinical practice.

1. Introduction

Over the past few decades, liver disease has become common worldwide, resulting in a mortality rate of 2 million deaths per year.[1,2] Liver dysfunction causes disordered bilirubin excretion, and subsequent hyperbilirubinemia often occurs due to bilirubin accumulation, leading to further deterioration of the disease and even death.[3] In addition to hyperbilirubinemia, endotoxemia is another severe complication associated with liver disease, *e.g.*, hepatitis,[4] fibrosis/cirrhosis,[5,6] and hepatocellular carcinoma.[7] In these liver diseases, Kupffer cells and liver sinusoidal endothelial cells cannot eliminate endotoxin (also called lipopolysaccharide, LPS) in the body, resulting in endotoxemia, organ disorders, and even death.[8,9]

In clinical practice, hemoperfusion is one of the most useful strategies for blood purification. This strategy has been utilized as a vital treatment for liver disease,[10–12] effectively improving the survival rate of patients.[13] Resin, a spherical polymer with a porous structure and high specific surface area, is widely applied as an adsorbent in hemoperfusion.[14] For example, the adsorbent polystyrene-divinylbenzene (PS-DVB) anion exchange resin shows strong bilirubin detoxification and a fast adsorption rate and has been commercially applied by Asahi Kasei Co., Japan.[15] However, most of the current adsorbents exploited for the treatment of hepatitis target the removal of a single toxin, bilirubin,[16,17] and endotoxin clearance has rarely been considered. Incomplete removal of toxins will result in poor therapeutic effects.[18]

To overcome this chronic problem, we prepared novel polymyxin B (PMB)-engineered polystyrene-divinylbenzene microspheres, as shown in Fig. 1. PMB is a cyclic and highly cationic decapeptide derived from *Bacillus polymyxa*.[19,20] The endotoxin–PMB complex is very stable and has an association constant (K_a) ranging from 1.8×10^{-6} to 2.3×10^{-6} M.[21] In the present study, we grafted 11-mercaptoundecanoic acid (MA) onto microspheres as a linker by thiol-ene click chemistry and then immobilized PMB to the surface *via* EDC/NHS coupling reactions. The scheme is illustrated in Fig. 2a. Considering the stable endotoxin–PMB interaction and the excellent bilirubin detoxification ability of PS-DVB microspheres, we expected that these novel microspheres could efficiently remove both bilirubin and endotoxin from patients.

2. Materials and methods

2.1 Materials

Endotoxin standards, chromogenic end-point *Tachypleus* Amebocyte Lysate (TAL) for endotoxin detection and endotoxin-

[a]School of Materials Science and Engineering, South China University of Technology, Guangzhou 510006, China. E-mail: psliren@scut.edu.cn
[b]National Engineering Research Center for Tissue Restoration and Reconstruction, South China University of Technology, Guangzhou 510006, China
[c]Key Laboratory of Biomedical Engineering of Guangdong Province, South China University of Technology, Guangzhou 510006, China
[d]Key Laboratory of Biomedical Materials and Engineering of the Ministry of Education, South China University of Technology, Guangzhou 510006, China
[e]Bioland Laboratory (Guangzhou Regenerative Medicine and Health Guangdong Laboratory), Guangzhou 510005, China
[f]Innovation Center for Tissue Restoration and Reconstruction, South China University of Technology, Guangzhou 510006, China

† Electronic supplementary information (ESI) available. See DOI: 10.1039/d1ra06684f

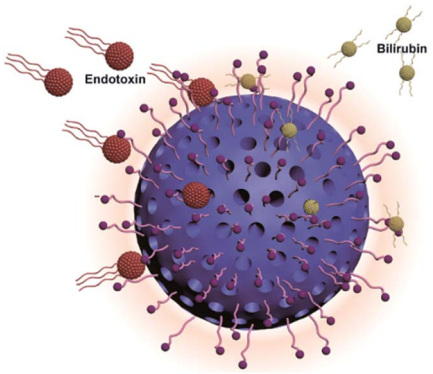

Fig. 1 Scheme of polymyxin B engineered polystyrene-divinylbenzene microspheres adsorbent for bilirubin and endotoxin removal.

free water were purchased from Xiamen Horseshoe Crab Reagent Manufactory (Xiamen, China). Bilirubin was purchased from Aladdin Bio-Chem Technology Co., Ltd (Shanghai, China). Anticoagulated rabbit blood and rabbit serum were purchased from Hongquan Biotechnology Co., Ltd (Guangzhou, China). Mouse embryonic fibroblast cells (L929) and human umbilical vein endothelial cells (HUVECs) were obtained from the American Type Culture Collection (ATCC; MD, USA). Cell counting kit-8 (CCK-8) was purchased from Dongren Chemical Technology Co., Ltd (Japan). Dulbecco's modified essential medium (DMEM), fetal bovine serum (FBS) and penicillin-streptomycin liquid were purchased from Gibco BRL Co. Ltd (CA, USA).

Polystyrene-divinylbenzene microspheres (PS-DVB microspheres; the diethylbenzene content was greater than 79%, and the content of hanging double bonds was 2.2–3.1 mmol g^{-1}) were provided by Guangdong Baihe Medical Devices Group Co., Ltd (Guangzhou, China), and 11-mercaptoundecanoic acid (MA, 98%) and PMB were obtained from Sigma Chemical Co., Ltd (MO, USA). Phosphate-buffered saline (PBS) was purchased from Solarbio Technology Co., Ltd (Beijing, Chain). 2,2-dimethoxy-2-phenylacetophenone (DMPA) and *N*,*N*-dimethylformamide (DMF) were purchased from Aladdin Bio-Chem Technology Co., Ltd (Shanghai, China). *N*-Hydroxysuccinimide (NHS) and *N*-(3-dimethyl-minopropyl)-*N*′-ethylcarbodiimide hydrochloride (EDC HCl) were purchased from Shanghai Macklin Biochemical Co., Ltd (Shanghai, China). Ethanol absolute was purchased from Guangshi reagent Technology Co., Ltd (Zhaoqing, China). All other materials and solvents were of analytical reagent grade.

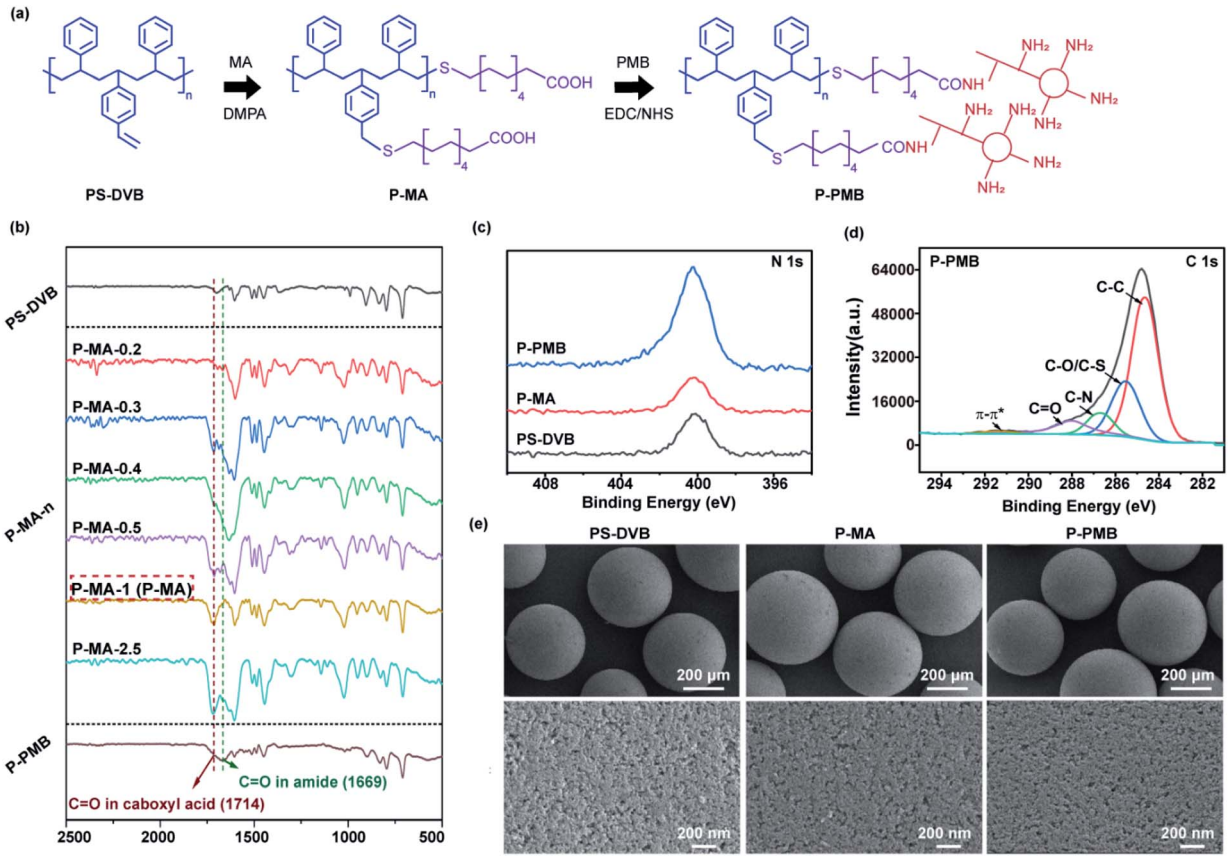

Fig. 2 (a) Scheme of the P-PMB microspheres prepared by thiol-ene click chemistry and EDC/NHS coupling reactions. (b) The FTIR spectra of different microspheres. (c) XPS N 1s high-resolution spectra of PS-DVB, P-MA and P-PMB microspheres. (d) XPS C 1s high-resolution spectra of P-PMB microspheres. (e) SEM images of the indicated microspheres at 50x and 300 00x magnifications.

2.2 Preparation of the engineered microspheres

MA (0.92–11.45 mmol) and DMPA (0.15 g, 0.59 mmol) were mixed with PS-DVB (1 g) in DMF (50 mL) in a sealed glass vial. The samples were shielded with aluminium foil while purged with nitrogen gas for 30 min. With the aluminium foil removed, the samples were exposed to 365 nm light at room temperature (~20 °C) for 1 h before being exposed to air. Then, the microspheres were washed with ethanol and endotoxin-free water separately for 1 day and dried in a vacuum drying oven (DP33C, Yamato, Japan) for 2 days at 40 °C. According to PS-DVB : MA ratios of 0.2 to 2.5, the samples were referred to as P-MA-0.2, P-MA-0.3, P-MA-0.4, P-MA-0.5, P-MA-1, and P-MA-2.5, where the number corresponds to the ratio in the sample.

Then, P-MA-1 (500 mg) was activated with EDC (388 mg, 2 mmol) and NHS (234 mg, 2 mmol) in PBS (20 mL) at room temperature for 1 h. The pH of the mixture was adjusted to 5.0 by 0.1 M HCl. Next, the microspheres were cleaned with PBS and mixed with PMB (80 mg, 0.06 mmol) in PBS (20 mL). The mixture was stirred for another 24 h. The microspheres were washed with PBS and endotoxin-free water separately for 1 day and then dried in a vacuum drying oven for 2 days at 40 °C.

2.3 Characterization

An FTIR assay was performed by a spectrometer (VERTEX 70, Bruker, Germany) with scanning from 4000 to 400 cm^{-1} at room temperature. Elemental analysis was performed by an elemental analyzer (UNICUBE, Elementar, Germany) to determine the contents of carbon, hydrogen, sulfur and nitrogen in the synthesis process of P-PMB microspheres. The –COOH content was calculated according to the corresponding S content. XPS spectra were obtained by an X-ray photoelectron spectrometer (ESCALAB™ Xi+, Thermo Scientific™, USA) employing Al Kα excitation radiation. Scanning electron microscopy (Nova Nano SEM 430, FEI, USA) was used to study the morphology of the microsphere surface. Prior to analysis, samples were dried and coated with gold. N_2 adsorption/desorption measurements were performed by an automatic gas adsorption analyzer (Autosorb iQ, Quantachrome Instruments, USA). The samples were degassed for 6 h at 120 °C. The specific surface area (SSA) was determined by the multipoint Brunauer–Emmett–Teller (BET) method using the adsorption data in the relative pressure range of 0.05 to 0.35. The pore size distribution and pore volume were calculated from the desorption isotherm using the density functional theory (DFT) method.

2.4 Biocompatibility assay

L929 and HUVECs were cultured in DMEM with 10% fetal bovine serum and 1% penicillin–streptomycin liquid at 37 °C in a 5% CO_2 incubator. Before cell seeding, the materials were immersed in the medium for 24 h at 37 °C (100 mg in 1 mL DMEM). Then, extract solutions were sterilized by passage through 0.22 μm filter membranes. The cells were seeded in a 96-well plate at a density of 10^4 cells per well with culture medium. After 24 h, the medium was replaced with fresh culture medium in the control group and with the extraction liquid in the experimental group. After culturing for another 24 h, cell cytotoxicity was characterized using a CCK-8 kit in accordance with the manufacturer's instructions.

2.5 Hemolysis analysis

According to the pharmaceutical industry standard of the People's Republic of China (YY/T 1651.1-2019), 8 mL sodium citrate anticoagulated rabbit blood was added to 10 mL normal saline to prepare diluted blood. Fifty milligrams of microspheres were incubated with 1 mL normal saline at 37 °C for 30 min. We employed normal saline and distilled water without microspheres as the negative and positive controls, respectively. Then, 20 μL of diluted blood was added to each tube and gently mixed. All tubes were incubated in a water bath at 37 °C for 60 min. The supernatant solution was obtained after centrifugation (800 g for 5 min) and measured at 545 nm by a multimode microplate reader (Varioskan™ LUX, Thermo Scientific™, USA). The hemolysis rate was calculated as follows:

$$\text{Hemolysis rate}(\%) = \frac{(OD_t - OD_{nc})}{(OD_{pc} - OD_{nc})} \times 100 \quad (1)$$

where OD_t, OD_{pc}, and OD_{nc} are the absorbance of the samples, positive control, and negative control, respectively.

2.6 Coagulation test

To evaluate the antithrombogenicity of the microspheres, a coagulation test was carried out. Briefly, 9 mL of blood from New Zealand rabbits was mixed with 1 mL of 3.8% sodium citrate. The fresh blood was centrifuged at 4000 rpm for 10 min to obtain platelet-poor plasma. Then, 1 mL of the resulting plasma was mixed with 50 mg of microspheres. After incubation at 37 °C for 30 min, the activated partial thromboplastin time (APTT), prothrombin time (PT), thrombin time (TT) and fibrinogen (FIB) level of the plasma were evaluated by a blood coagulation analyzer (Emo Express, Stago, France). The group without samples was served as the control.

2.7 Protein adsorption

To evaluate the protein adsorption capacity of microspheres in plasma, 500 mg adsorbents were incubated in 10 mL rabbit serum at 37 °C for 2 h. The total protein (TP) was analyzed using an automated biochemistry analyzer (3100, Hitachi, Tokyo, Japan).

2.8 Dynamic adsorption of toxins in plasma

Dynamic adsorption of endotoxin in rabbit plasma was evaluated by the TAL (chromogenic) method.[22] Briefly, 0.5 g of microsphere adsorbents were packed into a chromatography column (with an inner diameter of 1.5 cm and adjustable height of 25–155 mm) to simulate the hemoperfusion apparatus. Each time before use, the column was cleaned by perfusion with normal saline and endotoxin-free water. Then, 10 mL of plasma with endotoxin (2 EU mL^{-1}) was cycled through the column for 2 h at a flow rate of 4 mL min^{-1} by a constant current pump

(BT1-100L-LCD, Shanghai Qite Analytical Instrument Ltd, China). Plasma samples were collected at 0-, 10-, 30-, 60-, 90- and 120 min intervals. The amounts of adsorbed endotoxin at different times were investigated by a bacterial endotoxin detector (LKL-02-64, Zhanjiang A&C Biological Ltd, China).

Bilirubin adsorption was investigated in a similar manner. Briefly, 200 mg L^{-1} bilirubin solution was prepared in rabbit plasma to mimic the blood of hyperbilirubinemia patients. Plasma samples were collected at 0-, 10-, 30-, 60, 90-, 120- and 180 min intervals. Then, the bilirubin concentration was measured at 438 nm on a multimode microplate reader (Varioskan™ LUX, Thermo Scientific™, USA).

The endotoxin or bilirubin removal rate was calculated according to the following equation:

$$\text{Removal rate}(\%) = \frac{(C_0 - C_t)}{C_0} \times 100 \quad (2)$$

where C_0 (EU mL^{-1}) and C_t (EU mL^{-1}) are the initial and residual toxin concentrations at the indicated time points, respectively.

3. Results and discussion

First, we demonstrated that MA and PMB molecules were successfully immobilized on PS-DVB microspheres. The FTIR results (Fig. 2b) showed that compared to pristine PS-DVB microspheres, the MA-engineered microspheres (P-MA-*n*, where *n* is the ratio (0.2 to 2.5) in the reaction system) showed a new peak at 1714 cm^{-1}, which was attributed to the stretching vibrations of C=O in MA.[23,24] The increased intensity of the C=O peak demonstrated that the density of immobilized MA molecules was increased (P-MA-0.2 to P-MA-2.5). The results of the elemental analysis (Table S1†) were consistent with the FTIR results, where the P-MA-1 and P-MA-2.5 groups showed higher amounts of S than the other groups. Considering the amount of –COOH groups, we selected P-MA-1 (abbreviated as P-MA) to immobilize PMB *via* EDC/NHS coupling reactions for subsequent research. After the reaction, the FTIR spectrum of the PMB-engineered (P-PMB) microspheres showed a new peak at 1669 cm^{-1}, which was attributed to the amide C=O stretching vibration in PMB molecules.

The XPS N 1s and C 1s high-resolution spectra (Fig. 2c and d) showed obvious N (400.05 eV) and C=O (288.22 eV) peaks for P-PMB microspheres, further demonstrating the immobilization of PMB on microspheres.[25,26] Additionally, the elemental content results (Table S1†) showed that the N element increased from 0 to 1.41% in P-PMB microspheres compared to PS-DVB microspheres, which was consistent with the XPS results. According to the results, we calculated the amount of PMB grafted on the microspheres to be 87.2 mg g^{-1}.

Immobilization of MA and PMB did not influence the morphology and pore structure of the microspheres. The SEM images (Fig. 2e) showed that PS-DVB microspheres had a uniform spherical morphology and many nanosized pores. After immobilization of MA and PMB, the morphology of the microspheres did not obviously change. The N_2 adsorption–

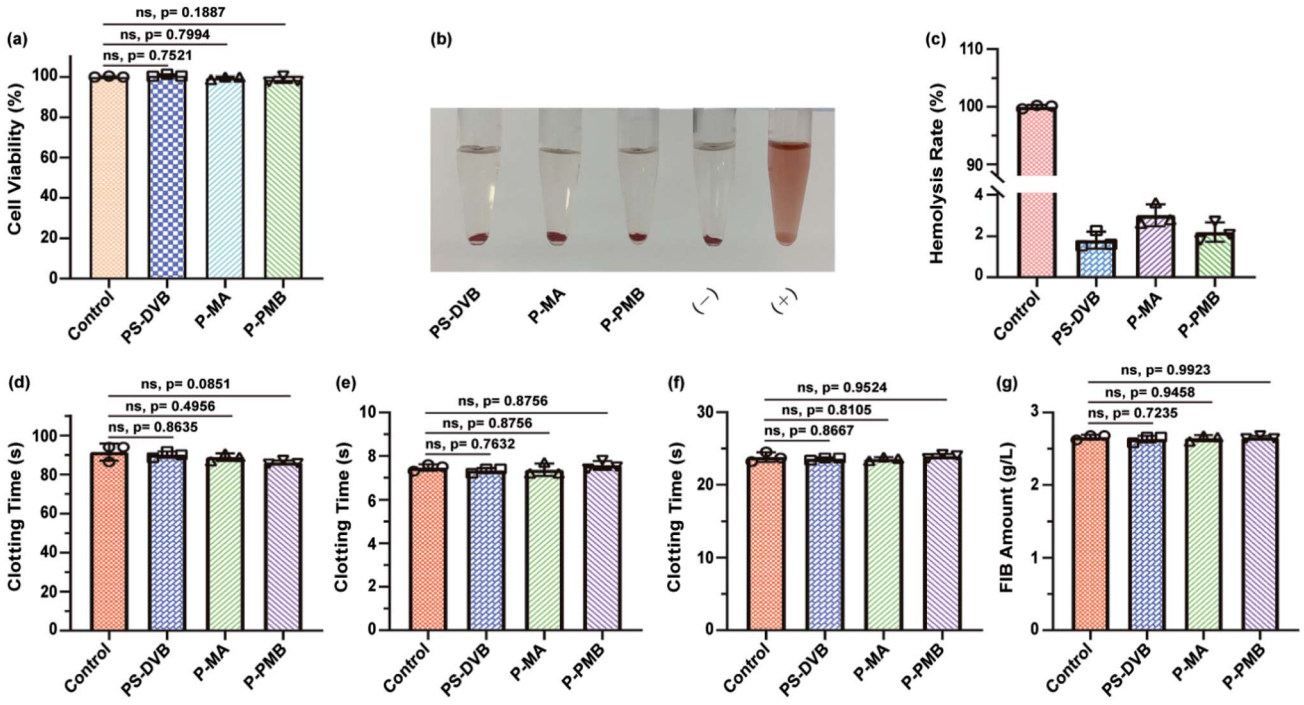

Fig. 3 (a) CCK-8 assay of the indicated microspheres in L929 cells ($n = 3$). (b) Visual observation of hemolysis in the extracts of the indicated microspheres. (−) was the negative control, and (+) was the positive control. (c) Hemolysis ratios of the extracts of the indicated microspheres. (d) Activated partial thromboplastin time, (e) prothrombin time, (f) thrombin time and (g) fibrinogen analyses of the PS-DVB, P-MA and P-PMB microspheres ($n = 3$).

desorption results (Fig. S2 and Table S3†) further illustrated that modification of the microspheres did not affect the diameters of the nanosized pores on the microspheres, which were 8.116, 8.219 and 8.195 nm on PS-DVB, P-MA and P-PMB microspheres, respectively. As previously reported,[27] the bilirubin adsorption of the microspheres mainly relied on pore size, and pores larger than 7 nm were desirable for PS-DVB adsorbents. The above results showed that the pore sizes of the microspheres were approximately 8 nm before and after modification, demonstrating that PMB immobilization did not affect bilirubin adsorption.

We demonstrated that the engineered microspheres had excellent biocompatibility and hemocompatibility. The cell counting kit-8 assay (CCK-8) results (Fig. 3a and S3†) showed that compared to the culture medium, the extracts of P-PMB microspheres showed negligible cytotoxicity to L929 and HUVECs, being similar to the other two types of microspheres (PS-DVB and P-MA). Meanwhile, the hemocompatibility results showed no visible hemolysis in the extracts of P-PMB microspheres (Fig. 3b). Quantitative analysis demonstrated that the hemolysis ratio of the P-PMB microspheres was only 2.20% (Fig. 3c), which was hemocompatible according to ISO 10993-5:1992 (less than 5%).[28] The hemocompatibility of the microspheres was further characterized by the anticoagulant property of the microspheres.

The *in vitro* clotting time results (Fig. 3d–f) showed that the APTT was slightly lower in the P-PMB microsphere group at approximately 96.00% than in the PS-DVB group ($p = 0.0851$). No significant differences in PT and TT were identified between the pristine PS-DVB and engineered P-PMB microspheres, demonstrating that the engineered microspheres had no effect on endogenous coagulation.[29] Additionally, both the pristine microspheres (PS-DVB) and the engineered microspheres (P-MA and P-PMB) had no effect on the adsorption of FIB (Fig. 3g). These results demonstrated the biosafety of the PMB-engineered microspheres during application; thus, these microspheres may have potential as blood-contact materials in hemoperfusion.

Protein comprising a net negative charge could interact with the ligand, thus competing with toxins for binding sites in plasma.[30–32] Therefore, the adsorption performance of microspheres toward protein was investigated in rabbit serum. The adsorption results of P-PMB microspheres showed that the total protein slightly decreased and was absorbed by 0.33 g L^{-1}, being similar to the other two microspheres (Fig. S4†). And the TP adsorption capacity of P-PMB microspheres was 6.6 mg g^{-1}, which was similar or lower than other reports.[33,34] And as reported, minor protein adsorption can be neglected as long as

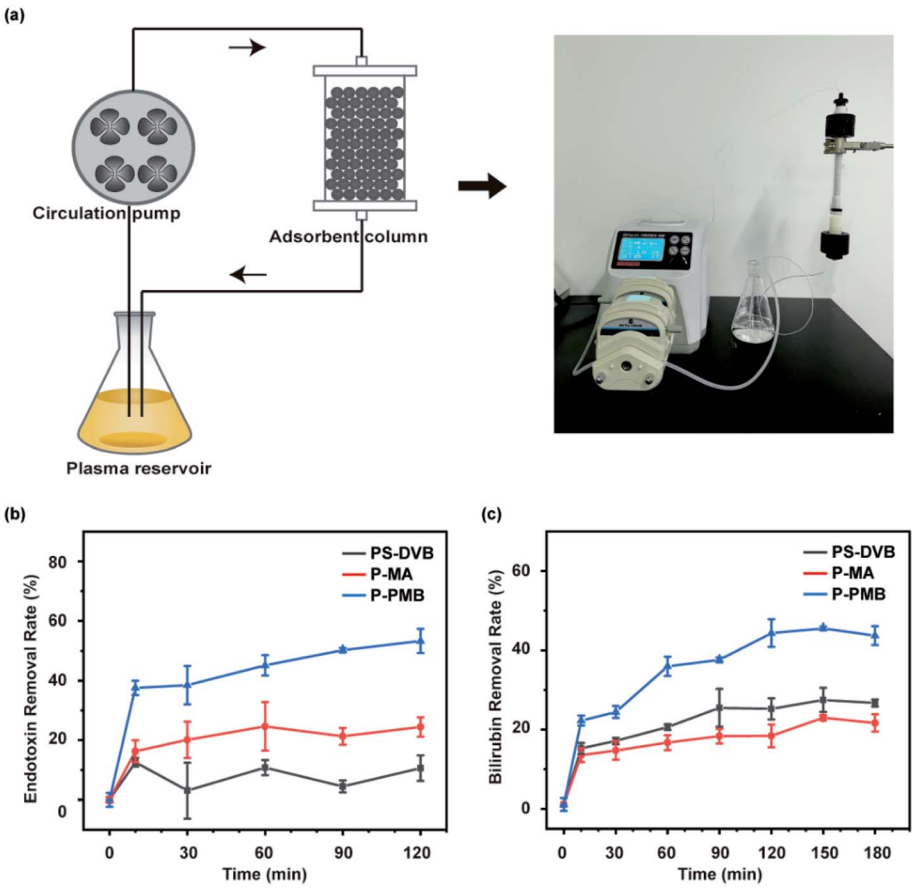

Fig. 4 (a) Schematic diagram and actual experimental diagram of the dynamic adsorption device. (b) Effects of adsorption time on the endotoxin removal rate in plasma. (c) Effects of adsorption time on the bilirubin removal rate in plasma.

the adsorption of toxins is ensured for hemoperfusion adsorbents.[35–37]

We performed dynamic adsorption simulation experiments on bilirubin or endotoxin in plasma (Fig. 4a), respectively. The dynamic adsorption of endotoxin results (Fig. 4b) showed that P-PMB microspheres had a strong endotoxin detoxification ability. There was a rapid adsorption process in 10 min for the P-MA and P-PMB microspheres owing to the frequent collisions between the exposed active sites and the large amount of endotoxin monomers.[38] After 120 min of adsorption, the endotoxin removal rate of P-PMB microspheres reached 53.35%, which was 5.03- and 2.18-fold higher than those of PS-DVB and P-MA microspheres, respectively. In patients with gram-negative sepsis, endotoxin clearance by a commercial product called PMX-F was only 47%,[39] which is slightly lower than that with our material, but no evidence indicated that PMX-F could remove bilirubin from plasma. PMB molecules have been reported to have positively charged amino groups that can bind to negatively charged phosphoric acid molecules on endotoxin molecules through electrostatic interactions,[40] and their long alkyl chains can bind to acyl hydrophobic chains on endotoxin by hydrophobic interactions. Due to these interactions, the P-PMB microspheres could adsorb more endotoxin than the other two types of microspheres.

Interestingly, in addition to endotoxin, the P-PMB microspheres also promoted bilirubin detoxification. The dynamic adsorption results (Fig. 4c) showed that for the three types of microspheres, the adsorption rate was rapid in the first 10 min, which was attributed to the rapid diffusion of bilirubin molecules into the pores on the microspheres.[41] As previously reported, PS-DVB microspheres adsorbed bilirubin through the nanopores on their surfaces.[42] Our results showed that modification of the microspheres did not affect their pore sizes (Table S3†). Therefore, all three types of microspheres could adsorb bilirubin through the pores. However, after MA modification, P-MA microspheres showed a negative charge and repelled negatively charged bilirubin. After 150 min, compared to that of PS-DVB microspheres, the bilirubin removal rate of P-MA microspheres decreased from 27.49% to 22.97%. After PMB modification, P-PMB microspheres exhibited a positive charge due to the five amino groups in PMB, which could strongly promote bilirubin adsorption by electrostatic interactions. P-PMB microspheres showed a maximum bilirubin removal rate of 45.56% after 150 min, which was 1.66- and 1.98-fold higher than those of PS-DVB and P-MA microspheres, respectively. In the presence of endotoxin in plasma, P-PMB microspheres still adsorbed bilirubin to some extent, and adsorbed bilirubin at a higher rate than the pristine PS-DVB microspheres (Fig. S5†). Additionally, the hemoperfusion time for clinical applications is usually 2–3 h,[43–45] being consistent with the time in our research, demonstrating that our microspheres could be stable for adsorbing toxins during application.

4. Conclusions

In summary, we developed novel PMB-engineered PS-DVB microspheres by thiol-ene click chemistry and EDC/NHS coupling reactions. These microspheres had excellent biocompatibility and hemocompatibility. Notably, compared to commercial PS-DVB microspheres, these engineered microspheres displayed stronger detoxification of both endotoxin and bilirubin, which are common toxins in liver disease. Considering the broad application prospects of PS-DVB microspheres in clinical practice and the remarkable detoxification ability of P-PMB microspheres, we believe that these novel microspheres will have considerable potential as absorbents in blood purification for liver disease.

Conflicts of interest

The authors declare that they have no known competing financial interests or personal relationships that could have appeared to influence the work reported in this paper.

Acknowledgements

This work was financially supported by the National Key R&D Program of China (2017YFC1104402, 2017YFC1105000, 2018YFC1105402, 2020YFB0204803), the Guangdong Province Key Field R&D Program Projects (2020B1111150002& 2019B010941002), the National Nature Science Foundation of China (Grants U1801252, 31771027), the Guangdong Natural Science Funds for Distinguished Young Scholars (2019B151502029), the Frontier Research Program of Bioland Laboratory (Guangzhou Regenerative Medicine and Health Guangdong Laboratory) (2018GZR110105008). L. W. thanks the Funds for Young Pearl River Scholars.

Notes and references

1 J. Xiao, F. Wang, N.-K. Wong, *et al.*, *J. Hepatol.*, 2019, **71**, 212–221.
2 P. Byass, *BMC Med.*, 2014, **12**, 159.
3 L. M. Guo, L. X. Zhang, J. M. Zhang, *et al.*, *Chem. Commun.*, 2009, 6071–6073.
4 A. Dolganiuc, O. Norkina, K. Kodys, *et al.*, *Gastroenterology*, 2007, **133**, 1627–1636.
5 R. Wiest and G. Garcia-Tsao, *Hepatology*, 2005, **41**, 422–433.
6 H. Fukui, *World J. Hepatol.*, 2015, **7**, 425–442.
7 N. Fatima, T. Akhtar and N. Sheikh, *Can. J. Gastroenterol. Hepatol.*, 2017, **2017**, 6238106.
8 J. P. Nolan, *Hepatology*, 2010, **52**, 1829–1835.
9 S. A. Faheem, N. M. Saeed, R. N. El-Naga, *et al.*, *Front. Pharmacol.*, 2020, **11**, 218.
10 G. Visco, R. Giannuzzi, M. G. Paglia, *et al.*, *Biomater., Artif. Cells, Immobilization Biotechnol.*, 1993, **21**, 265–281.
11 V. Dhokia, D. Madhavan, A. Austin, *et al.*, *J. Intensive Care Soc.*, 2019, **20**, 174–181.
12 M. Colaneri, P. Valsecchi, L. Perotti, *et al.*, *Liver Int.*, 2020, **40**, 2655–2659.
13 B. R. Müller, *Carbon*, 2010, **48**, 3607–3615.
14 Y. T. Yu, *Chin. Sci. Bull.*, 2013, **58**, 4357–4361.
15 G. L. Adani, D. Lorenzin, G. Currò, *et al.*, *Transplant. Proc.*, 2007, **39**, 1904–1906.

16 R. Senf, R. Klingel, S. Kurz, *et al.*, *Int. J. Artif. Organs*, 2004, **27**, 717–722.
17 R. Zhao, T. T. Ma, F. C. Cui, *et al.*, *Adv. Sci.*, 2020, **7**, 2001899.
18 R. Jalan, P. Gines, J. C. Olson, *et al.*, *J. Hepatol.*, 2012, **57**, 1336–1348.
19 B. Davies and J. Cohen, *Lancet Infect. Dis.*, 2011, **11**, 65–71.
20 X. Y. Zheng, Q. Cao, Q. Cao, *et al.*, *Chin. Chem. Lett.*, 2020, **31**, 413–417.
21 S. Srimal, N. Surolia, S. Balasubramanian, *et al.*, *Biochem. J.*, 1996, **315**, 679–686.
22 Z. X. Wang, B. Dong, Z. F. Feng, *et al.*, *BMC Immunol.*, 2015, **16**, 34.
23 Z. Lian, Y. Xu, J. Zuo, *et al.*, *Polymers*, 2020, **12**, 2157.
24 G. Premaratne, S. Farias and S. Krishnan, *Anal. Chim. Acta*, 2017, **970**, 23–29.
25 L. Qi, T. Pan, L. Ou, *et al.*, *Commun. Biol.*, 2021, **4**, 214.
26 Q. Dang, C. G. Li, X. X. Jin, *et al.*, *Carbohydr. Polym.*, 2019, **205**, 89–97.
27 V. Weber, I. Linsberger and M. Hauner, *Biomacromolecules*, 2008, **9**, 1322–1328.
28 Y. F. Zhou, B. Yang, X. Y. Ren, *et al.*, *Biomaterials*, 2012, **33**, 4731–4740.
29 J. W. Huang, X. Y. Zhang, Z. H. Wu, *et al.*, *J. Biomed. Nanotechnol.*, 2018, **14**, 98–113.
30 J. Chen, W. Han, R. Su, *et al.*, *Artif. Cells, Nanomed., Biotechnol.*, 2017, **45**, 174–183.
31 Q. Wu, Y. Xu, K. Yang, *et al.*, *J. Mater. Chem. B*, 2017, **5**, 8219–8227.
32 N. Gan, Q. Sun, L. Zhao, *et al.*, *J. Mater. Chem. B*, 2021, **9**, 5628–5635.
33 C. He, M. Li, J. Zhang, *et al.*, *Macromol. Biosci.*, 2020, **20**, e2000153.
34 S. Wu, B. Duan, X. Zeng, *et al.*, *J. Mater. Chem. B*, 2017, **5**, 2952–2963.
35 Q. Li, J. Yang, N. Cai, *et al.*, *J. Colloid Interface Sci.*, 2019, **555**, 145–156.
36 Z. Li, X. Huang, K. Wu, *et al.*, *Mater. Sci. Eng., C*, 2020, **106**, 110282.
37 Y. Liu, X. Peng, Z. Hu, *et al.*, *Mater. Sci. Eng., C*, 2021, **121**, 111879.
38 X. D. Cao, B. Y. Zhu, X. F. Zhang, *et al.*, *Carbohydr. Polym.*, 2016, **136**, 12–18.
39 T. Tojimbara, S. Sato, I. Nakajima, *et al.*, *Ther. Apheresis Dial.*, 2004, **8**, 286–292.
40 S. Vesentini, M. Soncini, A. Zaupa, *et al.*, *Int. J. Artif. Organs*, 2006, **29**, 239–250.
41 X. Song, J. L. An, C. He, *et al.*, *J. Mater. Chem. A*, 2019, **7**, 21386–21403.
42 Y. J. Wang and Y. T. Yu, *Artif. Cells, Blood Substitutes, Immobilization Biotechnol.*, 2011, **39**, 92–97.
43 Y. Chai, Z. Liu, Y. Du, *et al.*, *Bioact. Mater.*, 2021, **6**, 4772–4785.
44 A. Tyagi, Y. W. Ng, M. Tamtaji, *et al.*, *ACS Appl. Mater. Interfaces*, 2021, **13**, 5955–5965.
45 H. Fang, J. Wei and Y. Yu, *Biomaterials*, 2004, **25**, 5433–5440.